The Plant Cell, Vol. 23: 3671–3683, October 2011, www.plantcell.org © 2011 American Society of Plant Biologists. All rights reserved.

Auxin-Dependent Cell Cycle Reactivation through Transcriptional Regulation of *Arabidopsis E2Fa* by Lateral Organ Boundary Proteins [W]

Barbara Berckmans,[a,b] Valya Vassileva,[a,b,1] Stephan P.C. Schmid,[c] Sara Maes,[a,b] Boris Parizot,[a,b] Satoshi Naramoto,[a,b] Zoltan Magyar,[d] Claire Lessa Alvim Kamei,[a,b] Csaba Koncz,[e] Laszlo Bögre,[f] Geert Persiau,[a,b] Geert De Jaeger,[a,b] Jiří Friml,[a,b] Rüdiger Simon,[c] Tom Beeckman,[a,b] and Lieven De Veylder[a,b,2]

[a] Department of Plant Systems Biology, VIB, B-9052 Ghent, Belgium
[b] Department of Plant Biotechnology and Bioinformatics, Ghent University, B-9052 Ghent, Belgium
[c] Institut für Entwicklungsgenetik, Heinrich-Heine Universität Düsseldorf, D-40225 Duesseldorf, Germany
[d] Institute of Plant Biology, Biological Research Centre, H-6701 Szeged, Hungary
[e] Max-Planck-Institut für Züchtungsforschung, D-50829 Cologne, Germany
[f] Royal Holloway, University of London, Centre for Systems and Synthetic Biology, TW20 0EX Egham, United Kingdom

Multicellular organisms depend on cell production, cell fate specification, and correct patterning to shape their adult body. In plants, auxin plays a prominent role in the timely coordination of these different cellular processes. A well-studied example is lateral root initiation, in which auxin triggers founder cell specification and cell cycle activation of xylem pole–positioned pericycle cells. Here, we report that the E2Fa transcription factor of *Arabidopsis thaliana* is an essential component that regulates the asymmetric cell division marking lateral root initiation. Moreover, we demonstrate that *E2Fa* expression is regulated by the LATERAL ORGAN BOUNDARY DOMAIN18/LATERAL ORGAN BOUNDARY DOMAIN33 (LBD18/LBD33) dimer that is, in turn, regulated by the auxin signaling pathway. LBD18/LBD33 mediates lateral root organogenesis through *E2Fa* transcriptional activation, whereas *E2Fa* expression under control of the *LBD18* promoter eliminates the need for LBD18. Besides lateral root initiation, vascular patterning is disrupted in *E2Fa* knockout plants, similarly as it is affected in auxin signaling and *lbd* mutants, indicating that the transcriptional induction of *E2Fa* through LBDs represents a general mechanism for auxin-dependent cell cycle activation. Our data illustrate how a conserved mechanism driving cell cycle entry has been adapted evolutionarily to connect auxin signaling with control of processes determining plant architecture.

INTRODUCTION

As plants develop postembryonically, they produce continuously new structures in a flexible manner, allowing modifications in plant architecture in response to environmental conditions and specific needs. To model the body plan in accordance with external triggers, plant hormones, in particular auxin, play an important role (Friml, 2003; Tanaka et al., 2006; Vanneste and Friml, 2009). Auxin maxima can be found at organ initiation sites as well as in organs upon, for instance, gravity or light stimuli (Friml et al., 2002; Benková et al., 2003; Fuchs et al., 2003; Esmon et al., 2006; Traas and Monéger, 2010). A well-studied example of hormone-driven morphogenesis is root architecture that is determined by the number and placement of lateral roots (Overvoorde et al., 2010). In *Arabidopsis thaliana*, lateral root initiation is preceded by an oscillating auxin response in the basal meristem, priming the xylem-pole pericycle (XPP) as founder cells of lateral root primordia (De Smet et al., 2007; De Rybel et al., 2010; Moreno-Risueno et al., 2010). As they mature, these cells have the potential to undergo an asymmetric cell division, initiating the formation of a new lateral root. The subsequent cell divisions follow a well-organized pattern, resulting in lateral root emergence (Péret et al., 2009).

The molecular mechanism controlling lateral root initiation is based on the auxin-dependent degradation of INDOLE-ACETIC ACID INDUCED PROTEIN14 (IAA14)/SOLITARY ROOT (SLR), which leads to the derepression of AUXIN RESPONSE FACTOR7 (ARF7) and ARF19 (Fukaki et al., 2002; Okushima et al., 2005; Wilmoth et al., 2005). Both the gain-of-function mutant *slr-1* and the *arf7 arf19* double mutant abolish lateral root initiation. LATERAL ORGAN BOUNDARY DOMAIN16/ASYMMETRIC LEAVES2-LIKE18 (LBD16/ASL18), LBD29/ASL16, and LBD18/ASL20 were discovered as important constituents of the auxin signaling pathway operating downstream of ARF7/ARF19, as illustrated by their ability to partially complement the *arf7 arf19* lateral root phenotype upon overexpression (Okushima et al., 2007; Lee et al., 2009). The LBD proteins constitute a large family

[1] Current address: Institute of Plant Physiology and Genetics, Bulgarian Academy of Sciences, Academic Georgi Bonchev Street, Building 21, 1113 Sofia, Bulgaria.
[2] Address correspondence to lieven.deveylder@psb.vib-ugent.be.
The author responsible for distribution of materials integral to the findings presented in this article in accordance with the policy described in the Instructions for Authors (www.plantcell.org) is: Lieven De Veylder (lieven.deveylder@psb.vib-ugent.be).
[W] Online version contains Web-only data.
www.plantcell.org/cgi/doi/10.1105/tpc.111.088377

of plant-specific transcription factors, consisting of 43 family members in *Arabidopsis* (Shuai et al., 2002). Several members of this family have been linked with different auxin-regulated developmental processes, such as inflorescence architecture, embryogenesis, leaf patterning, vascular differentiation, male gametogenesis, and lateral root development (Shuai et al., 2002; Lin et al., 2003; Chalfun-Junior et al., 2005; Borghi et al., 2007; Soyano et al., 2008; Lee et al., 2009; Bureau et al., 2010; Oh et al., 2010). Therefore, identification of the downstream target genes of LBD transcription factors will aid in our understanding on how auxin signaling contributes to plant growth.

The establishment of a lateral root–inducible system allowed the identification of a whole subset of genes that are associated with lateral root initiation among which several are cell cycle–related genes, such as the B-type cyclin-dependent kinase (*CDK*) genes, the D-type cyclin *CYCD3;1*, Histone *H4*, and the *E2F* transcription factors (Himanen et al., 2002, 2004; Vanneste et al., 2005; De Smet et al., 2008). The latter is part of the E2F/DIMERIZATION PARTNER (DP)/RETINOBLASTOMA-RELATED (RBR) pathway that regulates the cell cycle initiation in a very conserved matter across higher eukaryotes. Upon the activation of G1/S-specific CDK/cyclin complexes, the transcriptional repressor RBR protein is hyperphosphorylated, resulting into its dissociation from the transcription factor E2F/DP that will activate the expression of several replication-specific genes (Inzé and De Veylder, 2006; Berckmans and De Veylder, 2009). *Arabidopsis* contains six E2F transcription factors that can be subdivided into classical (E2Fa, E2Fb, and E2Fc) and atypical (DEL1/E2Fe, DEL2/E2Fd, and DEL3/E2Ff), and two DPs (DPa and DPb). Whereas the atypical E2Fs appear to operate as inhibitors of a postmitotic event (Ramirez-Parra et al., 2004; Vlieghe et al., 2005; Lammens et al., 2008), the classical ones determine the division potential of cells. Both *E2Fa* and *E2Fb* are transcriptional activators of the cell cycle, and their overexpression causes enhanced cell proliferation (De Veylder et al., 2002; Sozzani et al., 2006). By contrast, *E2Fc* overexpression inhibits cell cycle progression; hence, E2Fc is seen as a repressor (del Pozo et al., 2002, 2006).

Here, using lateral root initiation as a model system, we uncovered a direct molecular link between auxin signaling and the cell cycle machinery. We show that E2Fa is rate limiting for lateral root primordia initiation. Moreover, we demonstrate that LBD proteins regulate the *E2Fa* expression, indicating that they steer auxin-dependent cell cycle activation through transcriptional induction of *E2Fa*.

RESULTS

E2Fa Is Involved in Lateral Root Initiation

As E2F transcription factors are well-known key regulators of cell cycle initiation, we examined whether the expression of any of the three classical E2F transcription factors of *Arabidopsis* correlated with lateral root initiation by means of available microarray data sets (Okushima et al., 2005; Vanneste et al., 2005; De Smet et al., 2008; Parizot et al., 2010). Synchronous lateral root initiation can be achieved through auxin treatment of roots pretreated with the auxin transport blocker 1-naphthylphthalamic acid (NPA) (Himanen et al., 2002, 2004; Vanneste et al., 2005; De Smet et al., 2008). In this system, seeds are germinated on medium containing NPA, inhibiting the formation of lateral root initiation sites. When seedlings are transferred after 3 to 4 d to medium with a high auxin concentration, lateral roots will be induced synchronously (Himanen et al., 2002).

In a microarray data set profiling the transcriptional changes upon auxin treatment, we noticed that within 2 to 6 h after naphthalene acetic acid (NAA) administration, coinciding with the G1/S transition and S phase initiation, a strong transcriptional activation of the *E2Fa* gene could be observed, whereas the expression levels of *E2Fb* and *E2Fc* genes remained relatively constant (Figure 1A). Auxin-dependent *E2Fa* expression was abolished in the *iaa14/slr-1* mutant, in which the auxin signaling leading to lateral root initiation is blocked (Figure 1B) (Fukaki et al., 2002). Moreover, microarray data resulting from green fluorescent protein (GFP)–based sorted cells from the J0121 enhancer trap line, which specifically labels the XPP cells (Casimiro et al., 2001), indicated that *E2Fa* is transcriptionally activated in the pericycle cells (Figure 1C). This result was confirmed by histochemical analysis of *ProE2Fa:GUS* (for β-glucuronidase) reporter lines (see Supplemental Figure 1A online). Correspondingly, a *ProE2Fa:E2Fa-GFP* line showed accumulation of the E2Fa protein in pericycle cell nuclei upon auxin treatment (Figures 1D and 1E). Furthermore, the E2Fa-GFP fusion protein was observed in neighboring migrating XPP nuclei, preceding the first asymmetric division that hallmarks lateral root initiation (Figures 1F and 1G). A role for E2Fa as initiator of lateral root initiation was confirmed by phenotypic analysis of two independent T-DNA insertion lines (see Supplemental Figures 1B to 1D online). In both lines, the absence of *E2Fa* transcripts correlated with a decrease in the number of primordia (emerged and nonemerged) (Figure 1H). Microscopy analysis revealed a significant reduction in the number of early-stage primordia (I, II, and III) (Figure 1I), consistent with a putative role for E2Fa in lateral root initiation. Together, these data suggest that cell cycle reactivation upon lateral root initiation is likely to be mediated through E2Fa activity.

LBD18 Binds the *E2Fa* Promoter and Is Induced upon Lateral Root Initiation

To identify the putative regulators regulating *E2Fa* expression upon lateral root initiation, we searched for transcription factors associating with the *E2Fa* promoter with the yeast one-hybrid method, which allows the identification of DNA–protein interactions. A 1364-bp promoter fragment of *E2Fa* was used as bait and screened against a cDNA library to isolate possible interactors. Two different transcription factors were found to bind to the *E2Fa* promoter: a Myb-like transcription factor (At1g25550) and the LBD18/ASL20 protein (hereafter designated as LBD18). Because of the known involvement of LBD proteins in the process of lateral root initiation, we focused on LBD18 that appeared to bind specifically the *E2Fa* promoter because it did not associate with the *E2Fb* and *E2Fc* upstream sequences (Figure 2A). Chromatin immunoprecipitation (ChIP) was used to confirm that LBD18 bound to the *E2Fa* promoter in vivo. Three different regions were assessed for LBD18 binding. Enrichment was observed by ChIP in a region 700 bp upstream of the ATG start codon in the *E2Fa* promoter (Figure 2B), correlating with the

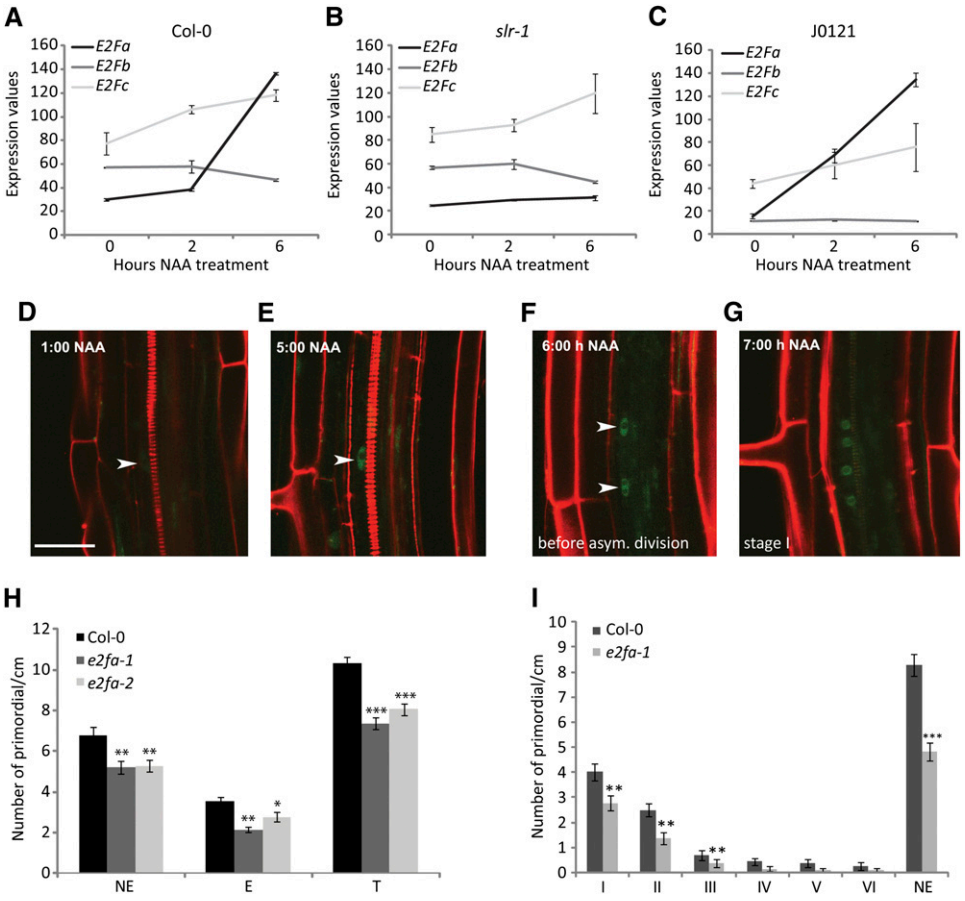

Figure 1. E2Fa Is Involved in Lateral Root Initiation.

(A) to **(C)** *E2Fa*, *E2Fb*, and *E2Fc* expression kinetics upon synchronous lateral root initiation in roots of Col-0 **(A)**, *slr-1* **(B)**, and in pericycle-sorted cells **(C)**. Data represent mean ± SE ($n \geq 2$).

(D) to **(G)** E2Fa-GFP protein accumulation upon NAA (5 μM) application after 1 h **(D)** or 5 h **(E)** in XPP cells counterstained with PI. E3Fa-GFP is visible before (6 h) **(F)** and after the first asymmetric division (7 h) **(G)** marking lateral root initiation. Bar = 50 μm (all photomicrographs are at the same magnification).

(H) Quantification of emerged (E), nonemerged (NE), and total (T) lateral root primordium density of *e2fa* T-DNA insertion lines 8 d after germination.

(I) Detailed staging of lateral root stage density of *e2fa* T-DNA insertion lines 8 d after germination. Data represent mean ± SE ($n \geq 12$; *P ≤ 0.05, **P ≤ 0.01, and ***P ≤ 0.001; two-sided *t* test).

presence of putative LBD binding sites (Husbands et al., 2007) (see Supplemental Figure 2 online).

Previously, LBD18 had been characterized as an auxin-dependent regulator of lateral root development, although, based on the phenotype of knockout lines, it was associated with lateral root outgrowth rather than with initiation (Lee et al., 2009). Using *ProLBD18*:*GUS* and *ProLBD18*:*NLS-GFP* reporter lines, we found that *LBD18* expression clearly correlated with asymmetric pericycle cell divisions (Figures 2C to 2E). Moreover, with the above-mentioned lateral root induction system, *LBD18* mRNA levels were induced upon NAA treatment (Figure 2F). This is in agreement with the expression data that could be extracted from the existing data sets that additionally revealed that the auxin-induced expression was dependent on IAA14/SLR and occurs in auxin-treated pericycle cells (see Supplemental Figures 3A to 3C online) (Vanneste et al., 2005; De Smet et al., 2008; Parizot et al., 2010). Additionally, transcript profiling of an *arf7 arf19* double mutant identified *LBD18* as a downstream target of the ARF7 and ARF19 pathway, as indicated by the lack of auxin inducibility of *LBD18* in the *arf7 arf19* double mutant (see Supplemental Figure 3D online) (Okushima et al., 2005; Parizot et al., 2010). Taking all these data together, we postulate that LBD18 plays a role in activating the cell cycle during de novo root formation by acting on *E2Fa* transcription.

LBD18 Cooperates with Other LBD Proteins during Lateral Root Development

The transcriptional activity of LBD18 on the *E2Fa* promoter was investigated by a transient activation assay in protoplasts.

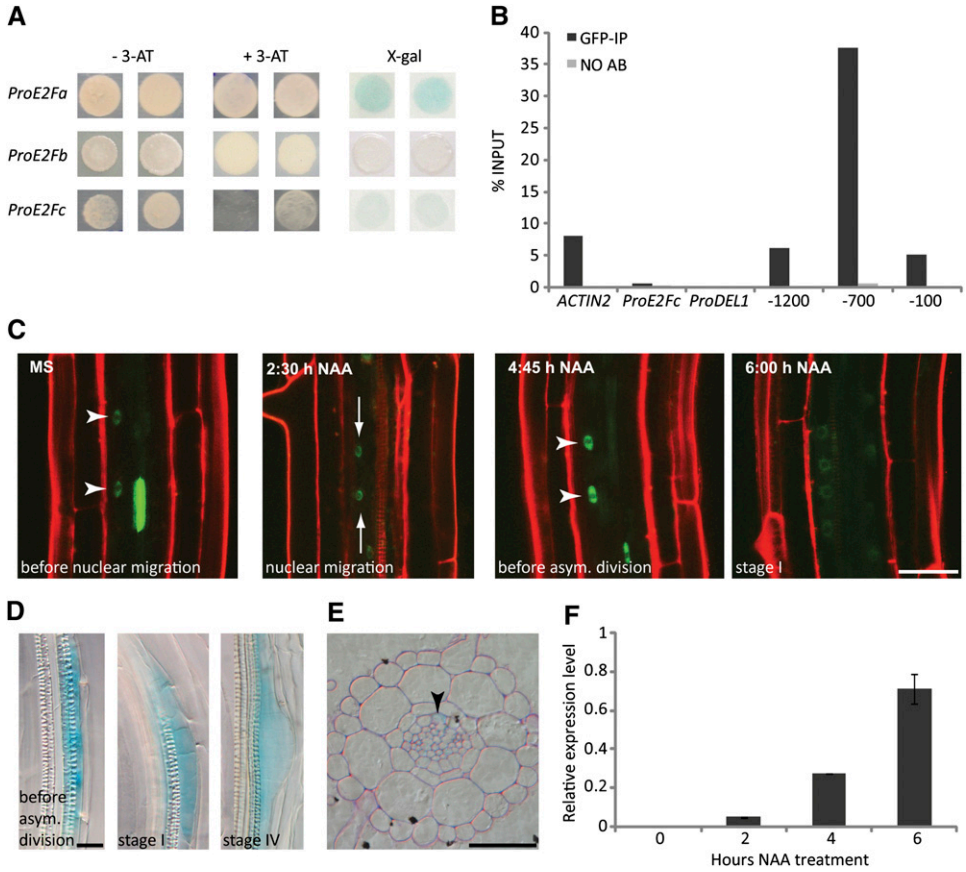

Figure 2. LBD18 Binds the *E2Fa* Promoter and Is Induced upon Lateral Root Initiation.

(A) and **(B)** Interaction of LBD18 with the *E2Fa* promoter in yeast **(A)** and in planta **(B)** as shown by yeast one-hybrid assay and ChIP, respectively. No association was observed with promoters of the closely related genes *E2Fb*, *E2Fc*, and *DEL1*. Interaction of LBD18 was truly positive when both *HIS3* (growth on 3-aminotriazole [+ 3-AT] medium) and *LacZ* (β-galactosidase [X-gal] positive) expression were induced.

(C) Confocal microscope images of *ProLBD18*:*NLS-GFP* counterstained with PI during lateral root initiation. Time of NAA treatment (5 μM) is indicated in the top left corner. Bar = 50 μm (all photomicrographs are at the same magnification).

(D) *ProLBD18*:*GUS* expression during different lateral root development stages: before asymmetric division (left), at stage I (middle), and at stage IV (right) . Bar = 50 μm (all photomicrographs are at the same magnification).

(E) Root cross section showing GUS staining in XPP cells. Bar = 50 μm.

(F) *LBD18* transcript accumulation upon synchronized lateral root initiation. Data are mean ± SE (n = 3).

Transient *LBD18* overexpression in protoplasts was not sufficient to induce the *E2Fa* promoter activity (Figure 3A). By contrast, when LBD18 was fused to the VP16 transcriptional activation or SRDX dominant repressor domain, *E2Fa* promoter activity was induced or repressed, respectively (Figure 3A). These data suggest that LBD18 on its own operates as a poor transcriptional regulator, probably requiring a cofactor to activate transcription. To identify such a factor, we used a tandem affinity purification (TAP) platform in cell cultures (Van Leene et al., 2007, 2010). *Arabidopsis* cell suspension cultures were stably transformed by *Agrobacterium tumefaciens*–mediated cocultivation with a *Pro35S*:*LBD18-TAP* cassette. On the basis of the presence of the double tag, a two-step affinity purification was performed. In total, five interacting proteins were identified, including another LBD protein, LBD33 (Table 1). By using fluorescence resonance energy transfer (FRET) measurements of the LBD18 and LBD33 versions tagged with fluorescent proteins, we could confirm the specific interaction between LBD18 and LBD33 in planta (Figure 4). Similarly to *LBD18* and *E2Fa*, *LBD33* expression was strongly upregulated in the lateral root induction system (Figure 3B). Furthermore, as seen for *LBD18*, this induction of *LBD33* was specific to the pericycle cells and depended on the IAA14/SLR and ARF7/19 pathway (see Supplemental Figure 3 online). Additionally, *lbd33* mutant plants displayed a strong reduction in lateral roots (Figure 3C). These data suggest that LBD18 and LBD33 might cooperate to drive *E2Fa* expression during lateral root initiation. Indeed, in contrast with LBD18 and LBD33 solely, coexpression of both *LBD* genes in protoplasts resulted in a significant activation of the *E2Fa* promoter activity, indicating that LBD18/LBD33 dimerization was necessary to drive *E2Fa* expression (Figure 3D).

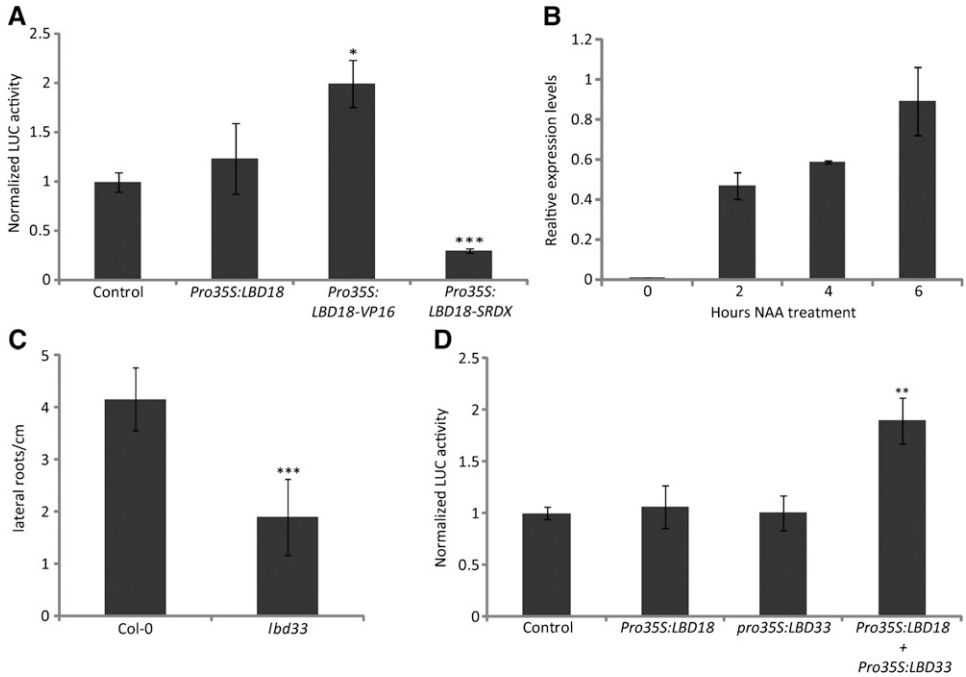

Figure 3. LBD18 Cooperates with the LBD33 Protein during Lateral Root Development.

(A) Protoplast transactivation activity assay with a *ProE2Fa:fLUC* reporter construct, a *Pro35S:rLUC* normalization construct, and an LBD18 effector construct that is either untagged (*Pro35S:LBD18*) or fused with VP16 (*Pro35S:LBD18-VP16*) or SRDX (*Pro35S:LBD18-SRDX*). Luciferase activity of control cells was arbitrarily set to 1. Data are means ± SE (n = 8; *P ≤ 0.05 and ***P ≤ 0.001; two-sided t test).
(B) *LBD33* expression upon synchronized lateral root initiation. Data are mean ± SE (n = 3).
(C) Lateral root density of control (Col-0) and *lbd33* knockout plants 8 d after germination. Data are mean ± SE ($n \geq 12$; ***P ≤ 0.001; two-sided t test).
(D) Protoplast transactivation activity assay with a *ProE2Fa:fLUC* reporter construct, a *Pro35S:rLUC* normalization construct, and LBD18 and/or LBD33 effector constructs. Luciferase activity of control cells was arbitrarily set to 1. Data represent mean ± SE (n = 8; **P ≤ 0.01; two-sided t test).

LBD18^{OE} in Combination with Auxin Induces Cell Division Capacity in Pericycle Cells

To investigate the link between LBD18 and cell cycle activation during lateral root initiation, GFP-tagged *LBD18* overexpression (*Pro35S:LBD18-GFP*) lines were generated. The LBD18-GFP fusion protein was functional because it was able to complement the *lbd18-2* lateral root phenotype. Transcript analysis on root segments of *Pro35S:LBD18-GFP* plants showed a modest increase in *E2Fa* expression (Figure 5A). Introducing a *ProE2Fa:GUS* reporter line into the *Pro35S:LBD18-GFP* background revealed that the increase in *E2Fa* expression was confined to

Table 1. Matrix-Assisted Laser Desorption/Ionization–Time-of-Flight/Time-of-Flight Mass Spectrometry Identification of LBD18 Interactors

Locus	Gene Description	Protein Molecular Weight	Peptide Count[a]	Sequence Coverage (%)	Protein Score[b]	E-Value	Best Ion Score[c]	E-Value
At3g11910	Ubiquitin-specific protease 13 (UBP13)	131,137	17	21	282	2.10E-24	50	1.70E-04
At5g06600	Ubiquitin-specific protease 12 (UBP12)	131,152	13	17	191	2.60E-15	51	2.00E-04
At3g10690	DNA Gyrase A	105,384	8	11	139	4.10E-10	52	1.30E-04
At5g06080	LOB domain–containing protein 33 (LBD33)	20,572	3	25	83	1.80E-04	44	6.80E-04
At5g24690	Protein of unknown function DUF3411	57,232	2	4	53	1.50E-01	49	4.10E-04

All proteins were detected in the two independent TAP experiments.
[a]The number of peptides with unique sequences matching the selected protein.
[b]Mascot score derived from the peptide mass fingerprint, combined with tandem mass spectrometry data.
[c]Ion scores are mascot scores from individual peptide sequence data.

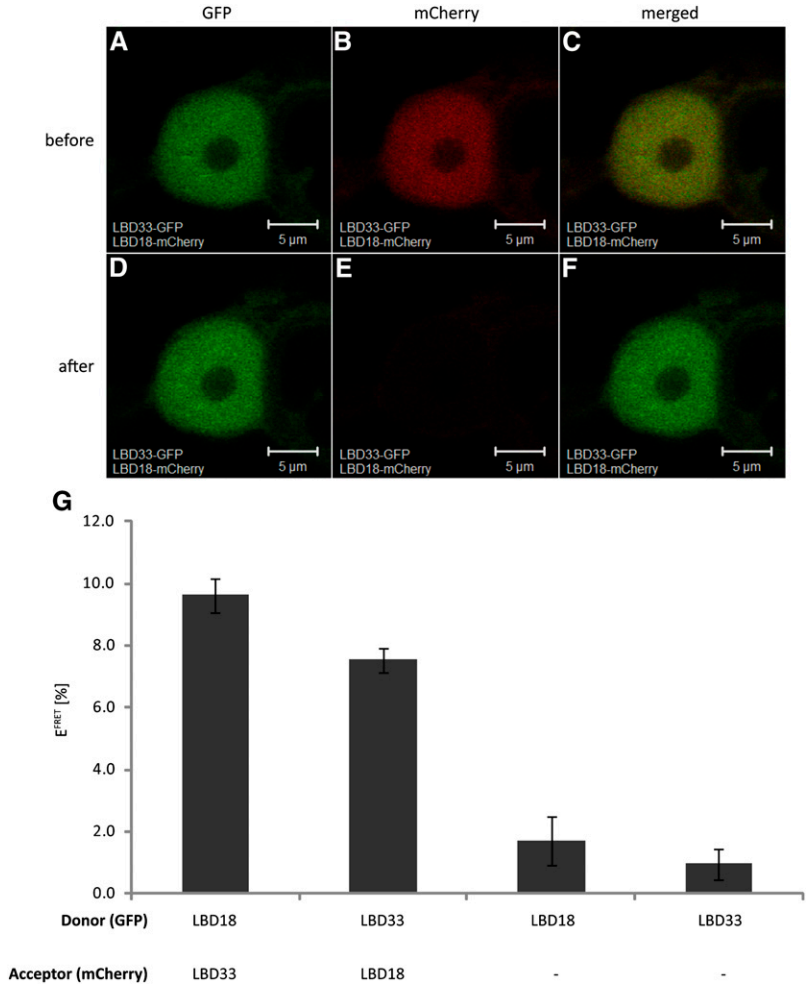

Figure 4. Confirmation of the LBD18–LBD33 Interaction by FRET Measurements.

(A) to **(F)** Confocal images of transgenic nuclei of *Nicotiana benthamiana* before (**[A]** to **[C]**) and after photobleaching of the acceptor (**[D]** to **[F]**). Fluorescence of the fusion proteins LBD33-GFP (donor) and LBD18-mCherry (acceptor) is shown in two channels for the GFP detection (497 to 550 nm) (**[A]** and **[D]**), mCherry detection (572 to 636 nm) (**[B]** and **[E]**), and merged (**[C]** and **[F]**). Bars = 5 μm.

(G) FRET efficiency (E_{FRET}) values in percentages. Donor and acceptor are fusion proteins composed of an LBD protein and the fluorophore GFP and the fluorophore mCherry, respectively. Negative controls are fusions of an LBD protein and GFP alone; corresponding values are considered background noise. Data represent mean ± SE ($n \geq 12$).

pericycle cells and was not visible in any other tissue type (Figures 5B to 5E), indicating that *E2Fa* regulation by LBD18 was highly specific to the pericycle cells. However, whereas the *lbd18* knockout reduces lateral root density, the overexpression of *LBD18* did not yield the expected increase in lateral roots under standard growth conditions. Rather, a decrease in primordia density was observed (Figure 5F), which probably can be explained by the dramatic effect of *LBD18* overexpression on vascular differentiation (Soyano et al., 2008). Moreover, previously it had been postulated that cell division on its own was insufficient to induce lateral roots because of the lack of a lateral root specification factor (Vanneste et al., 2005; De Smet et al., 2010). Therefore, wild-type and *Pro35S:LBD18-GFP* seeds were germinated on control medium and subsequently transferred to medium supplied with 0.5 μM NAA for 4 d. Quantification of lateral root primordia revealed that addition of NAA resulted in an increase in the number of primordia in the *LBD18-GFP* overexpressing lines when compared with the wild type (Figure 5F). Closer examination of the root tissues revealed hyperplasia of the transgenic pericycle cells (Figures 5G and 5H), which correlated with a strong transcriptional activation of the *E2Fa* promoter (Figures 5I and 5J). Additionally, expression of *E2Fa* under the control of the *LBD18* promoter rescued the lateral root phenotype of *lbd18* mutant plants (Figure 5K), demonstrating that *E2Fa* transcription can shortcut the need for LBD18.

E2Fa^{KO} Plants Show a Reduced Vascular Complexity

Our data raise the hypothesis that *E2Fa* could be an important target used by auxin to connect developmental patterning

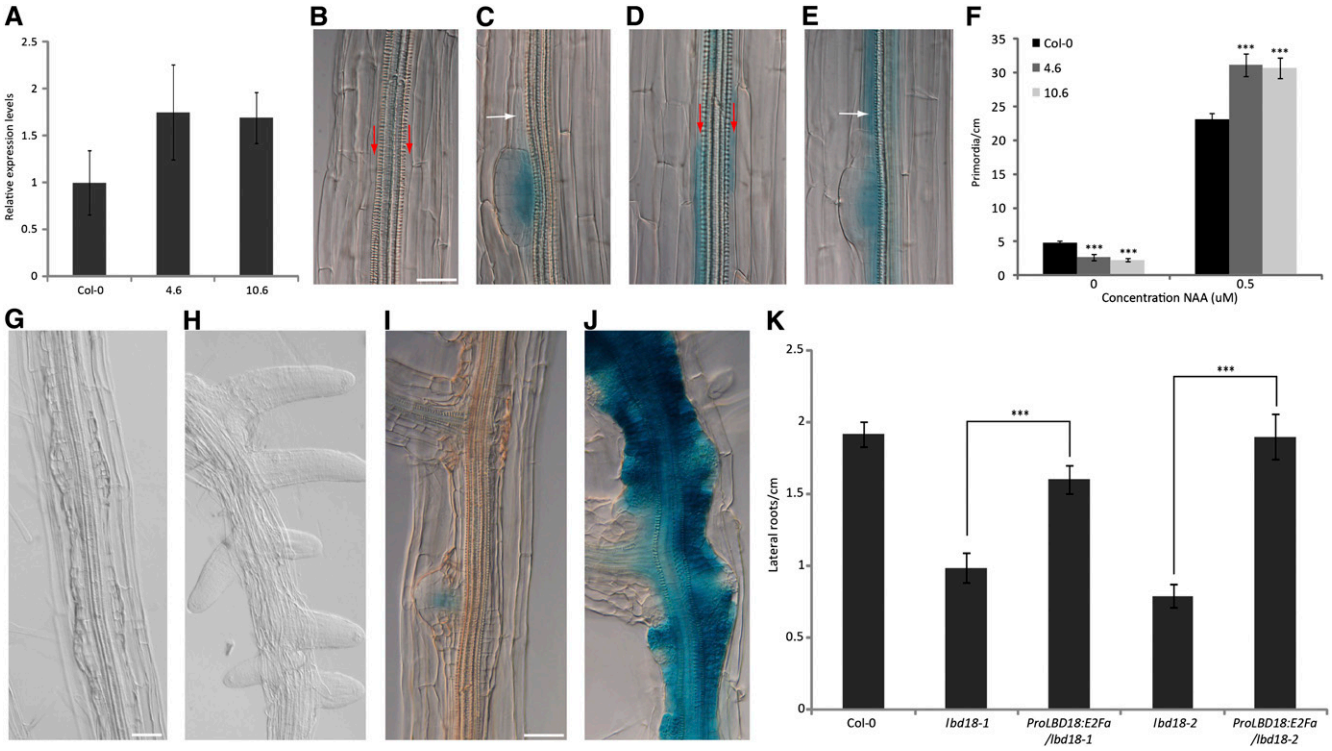

Figure 5. *LBD18* Overexpression Induces *E2Fa* Expression in Pericycle Cells and Hyperplasia upon Auxin Treatment.

(A) *E2Fa* expression levels in roots of control (Col-0) and *Pro35S:LBD18-GFP* lines 4.6 and 10.6. Data represent mean ± SD ($n = 3$).
(B) to **(E)** *ProE2Fa:GUS* expression in Col-0 (**[B]** and **[C]**) versus *Pro35S:LBD18-GFP* (**[D]** and **[E]**) plants. Red and white arrows mark enhanced *GUS* expression in pericycle cells and pericycle cells flanking lateral root primordia, respectively. Bar = 50 μm (all photomicrographs are at the same magnification).
(F) Lateral root density in 8-d-old seedlings that were transferred 4 d after germination to medium supplemented with DMSO or 0.5 μM NAA for an additional 4 d. Data represent mean ± SE ($n \geq 12$;***$P \leq 0.001$; two-sided *t* test).
(G) and **(H)** Root phenotypes of control (Col-0) **(G)** and *35S:LBD18-GFP* **(H)** after transfer for 4 d to medium supplemented with 1 μM NAA. Bar = 50 μm (all photomicrographs are at the same magnification).
(I) and **(J)** *E2Fa* expression in Col-0 **(I)** and *Pro35S:LBD18-GFP* **(J)** after transfer for 4 d to medium supplemented with 1 μM NAA. Bar = 50 μm (all photomicrographs are at the same magnification).
(K) Lateral root density in Col-0, *lbd18-1*, *lbd18-2*, and both lines complemented with the *ProLBD18:E2Fa* construct. Data represent mean ± SE ($n \geq 12$; *** $P \leq 0.001$; two-sided *t* test).

processes with cell cycle activation. As *E2Fa* was also expressed in the veins (Figure 6D), and vein pattern formation is known to require both organized auxin signaling and cell division, we analyzed the vascularity in $E2Fa^{KO}$ plants (Kang et al., 2007; Rolland-Lagan, 2008). Cotyledon vein structure is a simple and ideal model to test vascular complexity. Under normal conditions, the cotyledon vein consists of a primary middle vein and four additional secondary veins that form four closed loops. Interestingly, *E2Fa* mutants showed a reduced vascular complexity in the cotyledons (Figures 6A to 6C, Table 2). These data suggest that *E2Fa* is an important target for auxin to integrate cell cycle progression in auxin-mediated processes.

DISCUSSION

E2Fa Contributes to Lateral Root Initiation

Different transcript profiling studies show that the process of lateral root initiation coincides with the upregulation of different cell cycle genes, but, although several reports contributed to the knowledge of auxin-dependent lateral root initiation, how these signaling cascades impinge directly on the core cell cycle machinery remains unresolved. Here, we demonstrated that E2Fa could be responsible for triggering the first asymmetric division linked with lateral root ontogenesis. Not only did we observe that *E2Fa* transcripts and proteins accumulate before the onset of asymmetric division, but also that depletion of *E2Fa* significantly reduces the number of lateral root primordia. These data support the hypothesis that E2Fa could be a key target used by the auxin signaling pathway to connect developmental patterning processes with cell cycle activation.

Overexpression of *E2Fa* together with its dimerization partner *DPa* induces ectopic divisions at the whole-plant level, severely affecting plant development (De Veylder et al., 2002). Besides *E2Fa*, *Arabidopsis* possesses a second cell cycle–activating *E2F*, namely *E2Fb*, which also induces extra cell divisions when overexpressed (Sozzani et al., 2006). The presence of two activating E2F factors might explain why *E2Fa* depletion does

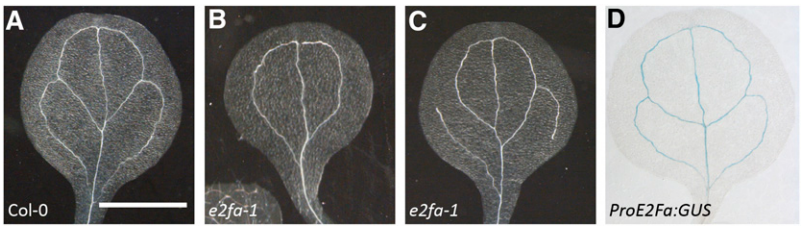

Figure 6. Aberrant Vascular Tissue Development in *E2Fa* Knockout Plants.

(A) Wild-type venations typically including three or four closed areoles.
(B) and **(C)** *E2Fa* knockout regularly causing fewer areoles **(B)** and disconnected veins **(C)**.
(D) *ProE2Fa*:*GUS* expression pattern in the vascular tissue.
Bar = 1 mm (all photomicrographs are at the at same magnification).

not completely inhibit lateral root formation. Although no significant increase in the *E2Fb* gene transcript level was observed upon auxin application, the E2Fb protein is detectable in the pericycle cells (see Supplemental Figure 4 online), where it might be activated posttranscriptionally upon auxin treatment (e.g., through release from the inhibitory RBR protein). Recently, the CYCD2;1/CDKA complex has been linked with lateral root initiation (Sanz et al., 2011). This complex accumulates in the nuclei of division-competent pericycle cells but is kept inactive through association with the CDK inhibitor KRP2. Upon auxin treatment, KRP2 is rapidly downregulated, both at the transcriptional and posttranscriptional levels (Himanen et al., 2004; Sanz et al., 2011). Hereby, the activity of the nuclear reservoir of CYCD2;1/CDKA complexes might be released, possibly resulting in hyperphosphorylation of RBR and thus activating E2Fb without the need for transcriptional induction. Correspondingly, an *e2fb* T-DNA insertion line showed a small, but significant, reduction in lateral root density, which is partially due to a decrease in the number of initiation events (see Supplemental Figure 5 online). In other words, different integrated pathways might control cell cycle activation linked to lateral root initiation.

LBD18 Links Auxin Signaling with Cell Cycle Activation during Lateral Root Initiation

The observed association of LBD18 to the *E2Fa* promoter, the coregulation of both genes during the lateral root initiation event, and the changes in *E2Fa* expression in *Pro35S*:*LBD18-GFP* plants all hint that LBD18 forms the missing link between the ARF7/ARF19 signaling cascade and cell cycle activation. Previously, overexpression of *E2Fa*/*DPa* has been reported to enhance the capacity of pericycle cells to induce lateral roots. Under standard growth conditions, the number of lateral roots in *E2Fa*/*DPa* overexpression lines is lower than that of control plants but significantly increases in the presence of auxin (De Smet et al., 2010). Interestingly, we saw a similar effect in the *Pro35S*:*LBD18-GFP* lines, possibly due to an increase in *E2Fa* transcript levels in the pericycle cells of these lines. However, overexpression of *E2Fa*/*DPa* resulted in stretches of small pericycle cells caused by ectopic cell division, which was not the case in the *Pro35S*:*LBD18-GFP* lines. Increased *ProE2Fa*:*GUS* activity within *Pro35S*:*LBD18-GFP* plants was not uniform across the whole pericycle, indicating that LBD18 can probably only activate *E2Fa* expression in pericycle cells that already contain the pericycle founder cell identity. Additional factors, besides LBD18, might be needed to induce the *E2Fa* promoter activity. In support for this hypothesis, LBD18 alone operates as a poor activator of *E2Fa* transcription in protoplast cells, and prolonged NAA treatment of *Pro35S*:*LBD18-GFP* plants results in hyperplasia of the whole pericycle, indicating that the limiting factor requires an auxin-dependent pathway.

LBD18 and LBD33 Coregulate Lateral Root Initiation

Here, LBD proteins were found to dimerize. Dimerization may occur through the Leu zipper–like sequences and might aid sequence-specific binding to LBD *cis*-acting elements or result in the formation of a transcriptional activation domain. Alternatively, dimerization might influence the interaction with other proteins, because LBD proteins have been previously shown to interact with basic helix-loop-helix proteins that control the LBD activity posttranscriptionally (Husbands et al., 2007).

Through a TAP purification experiment, we identified LBD33 as a LBD18-interacting protein. The specific induction of *LBD33* transcript levels upon lateral root initiation and the decrease in lateral root density in *lbd33* mutant plants make it a good candidate to cooperate with LBD18 in the process of *E2Fa* induction. Previously, LBD18 and LBD16 have been shown to probably work together in lateral root development (Lee et al., 2009). By means of VisuaLRTC, representing a compendium of publicly available microarray data sets linked to *Arabidopsis* lateral root development (Parizot et al., 2010), we found five genes (*LBD16*, *LBD17*, *LBD18*, *LBD29*, and *LBD33*) that were induced upon lateral root initiation in a SLR/ARF7/ARF19-dependent manner, of which *LBD16*, *LBD18*, and *LBD29* have been described previously to control outgrowth of lateral root primordia (Okushima et al., 2007; Lee et al., 2009). FRET analysis revealed that different LBD

Table 2. Variations of Cotyledon Vein Formation

Line	Normal Areoles	Reduced Areoles	Disconnected
Col-0	92.9% (78/84)	4.8% (4/84)	2.4% (2/84)
e2fa-1	54.5% (48/88)	36.4% (32/88)	9.1% (8/88)
e2fa-2	54.8% (40/73)	38.4% (28/73)	6.8% (5/73)

The venations that include three or more areoles and two areoles were defined as normal and reduced areoles, respectively.

complexes exist, besides the LBD18/LBD33 dimer. Various LBD combinations might act at different stages of lateral initiation and development of root primordia or might operate redundantly. Indeed, the absence of lateral root initiation phenotypes in *lbd16 ldb18* and *lbd18 lbd33* double mutants (Lee et al., 2009) (see Supplemental Figure 6 online) hints at functional redundancy between different LBD complexes in the regulation of the XPP cell cycle activation.

LBD Proteins and Cell Cycle Regulation

The LBD transcription factor family comprises 43 members in *Arabidopsis* (Shuai et al., 2002; Matsumura et al., 2009; Majer and Hochholdinger, 2011). Several studies have described the effect of *LBD* misregulation, showing that LBD proteins are seemingly involved in a remarkably diverse number of developmental processes, with phenotypes linked to defects in auxin response and/or cell proliferation. The first and best characterized *lbd* mutant, *asymmetric leaves2*/*LBD6*, shows abnormalities in leaf shape due to impaired abaxial/adaxial identity (Semiarti et al., 2001). The first visible effect of the phenotype is an asymmetric auxin response, followed by asymmetry in the cell division pattern and an increase in cell number in the adaxial domain (Zgurski et al., 2005; Iwakawa et al., 2007). Moreover, overexpression of *AS2* in tobacco (*Nicotiana tabacum*) cell cultures interrupted cell division (Iwakawa et al., 2007). In maize (*Zea mays*), the mutation in the *LBD* gene *indeterminate gametophyte1* restricts the proliferative phase in embryo sac development during female gametogenesis. Additionally, mutants exhibit abnormal leaf morphology due to persistent cell proliferation and maintenance of stem cell identity in the leaf cells (Evans, 2007). Recently, *SIDECAR POLLEN* encoding *LBD27*/*ASL29* has been shown to be necessary for the correct timing and orientation of asymmetric microspore division during male gametophyte development (Oh et al., 2010). The closest homolog of *LBD18*, *LBD30*, was characterized and designated *JAGGED LATERAL ORGANS* (*JLO*) (Borghi et al., 2007; Bureau and Simon, 2008; Bureau et al., 2010). *JLO* overexpression results in multiple phenotypes, including an early meristem arrest and lobbed leaves. Interestingly, a 24-h induction of *JLO* identified *CYCD3;1* and *CYCD3;2* as downstream induced genes (Borghi et al., 2007). In *JLO* overexpression plants, the trichome ploidy levels were up to 128C, whereas they were reduced in leaves, strengthening the link between *JLO* misexpression and cell cycle regulation. Moreover, *jlo* mutants show a certain degree of embryonic lethality that might be linked to aberration of early divisions during embryo development (Bureau et al., 2010). Furthermore, *jlo* mutants also exhibit a reduced vascular complexity in the cotyledons. It would be worthwhile to test whether it might be connected to the same phenotype observed in *e2fa* mutant plants. JLO could possibly work together with LBD18 that has been described previously to be involved in vascular differentiation as well (Lee et al., 2009).

All these phenotypic data imply that not only LBD18/LBD33, but also other LBD combinations, might steer cell division activity through transcriptional induction of *E2F* genes and/or other cell cycle genes, depending on the developmental context. As plants develop mostly postembryonically, they must be able to adapt their growth to changing external conditions. The ability to create new structures, such as lateral roots, through dedifferentiation of already differentiated plant cells provides a high level of plasticity. However, this plasticity requires connectivity between intrinsic development and external signals. Based on our data, we hypothesize that the plant-specific LBD proteins link auxin signaling with cell cycle initiation by regulating the *E2Fa* transcription. In contrast with the E2F/DP/RBR pathway that represents a highly conserved mechanism to drive cell cycle activation across all higher eukaryotes, auxin signaling seems to be specific to the plant lineage (De Smet et al., 2011). Therefore, our work indicates that during evolution, LBD proteins might have arisen in the plant kingdom to associate the highly conserved mechanism of cell cycle activation with plant-specific hormone signaling.

METHODS

Plant Materials and Growth Conditions

Arabidopsis thaliana strain Columbia (Col-0) and the following T-DNA insertion lines were analyzed: SALK_038125 (*lbd18-1*), SAIL_269_H02 (*lbd18-2*), SAIL_95_H10 (*lbd33*), GABI_348E09 (*e2fa-2*), and MPIZ-244 (*e2fa-1*) obtained from the collection of the Max-Planck-Institut für Züchtungsforschung of Cologne (Ríos et al., 2002) and SALK_103138 (*e2fb*). Primer sequences used for genotyping are given in Supplemental Table 1 online. For lateral root-related experiments, plants were grown on vertical square plates (Greiner Labortechnik) with solid half-strength Murashige and Skoog (MS) medium supplemented with 0.5 g/L MES, 10 g/L Suc, and 1% plant tissue culture agar. The plates were incubated at 4°C for 48 h to synchronize seed germination. Seedlings were incubated under continuous light (110 μEm^{-2} s^{-1} PAR, supplied by cool-white fluorescent tungsten tubes; Osram) at 22°C. For the NPA/NAA-mediated lateral root induction system, 5-d-old seedlings were transferred for 2, 4, or 6 h from MS with 10 μM NPA (the auxin-transport blocker) to MS with 10 μM NAA (the synthetic auxin analog) as described (Himanen et al., 2002). For the auxin treatment of *Pro35S*:*LBD18-GFP* lines, seeds were germinated on MS for 4 d and transferred to MS medium supplemented with DMSO or 0.5 μM NAA for 4 d. For all other experiments, seedlings were grown in horizontal plates and incubated under 16-h/8-h day/night conditions at 22°C.

Cloning and Generation of Transgenic Lines

Standard molecular biology protocols and Gateway (Invitrogen) technology were followed to obtain expression clones. Open reading frames (ORFs) were amplified from a cDNA template with Pfu DNA Polymerase (Promega) and fused to Gateway attB sites by PCR. For promoter isolation, genomic DNA was used as source. Primer sequences used are given in Supplemental Table 2 online. pdonr221 and p4-p1r were used as ENTRY vectors respectively. The structure and sequence of all destination vectors were as described (Karimi et al., 2002, 2007) and are available online at http://www.psb.ugent.be/gateway/ or otherwise referenced. For promoter analysis of *LBD18*, a 2-kb fragment upstream of the start codon was cloned in the vector pMK7S*NFm14GW, generating the *ProLBD18*:*NLS-GFP-GUS* construct, resulting in the transcriptional fusion between the *LBD18* promoter and the *EGFP-GUS* fusion. *Pro35S*:*LBD18-GFP* was obtained by cloning the ORF of *LBD18* in the destination vector pH7FWG2, creating a fusion between *LBD18* and *EGFP*. *ProE2Fa*:*GUS* was generated through cloning of the *E2Fa* promoter in pKGWFS7. The *ProE2Fa*:*gE2Fa-GFP* translational fusion had been described previously (Henriques et al., 2010). Genetic complementation was assessed by transforming the *Pro35S*:*LBD18-GFP* construct in the *lbd18-2*

background or by transforming a *ProLBD18:E2Fa* construct in the pH7m24GW,3 vector in the *lbd18-1* and *lbd18-2* backgrounds. All transgenic plants were generated by the floral dip method (Clough and Bent, 1998). Both *lbd18-1* and *lbd18-2* had a reduced *LBD18* expression and showed the lateral root phenotype described previously (Lee et al., 2009).

Microarray Data Extraction

For the extraction of the values from the previously published arrays (Okushima et al., 2005; Vanneste et al., 2005; De Smet et al., 2008), the respective data sets were retrieved from the Gene Expression Omnibus (GEO GDS1515, GSE6349, and GSE630). The samples used from the transcriptomic experiment of Vanneste et al. (2005) were GSM75508, GSM75509, GSM75510, GSM75512, GSM75513, GSM75514, GSM75516, GSM75517, GSM75518, GSM75519, GSM75520, and GSM75521, which corresponded to three or two replicates (for the time points 0 h control and 2 and 6 h after treatment, respectively) for the two genotypes (Col and *slr*). The samples used from the transcriptomic experiment of De Smet et al. (2008) were GSM146819, GSM146822, GSM146818, GSM146821, GSM146820, and GSM146823, which corresponded to two replicates for each time point (before treatment and 2 and 6 h after treatment). The samples used from the transcriptomic experiment of Okushima et al. (2005) were GSM9571, GSM9572, GSM9573, GSM9574, GSM9575, GSM9576, GSM9577, GSM9578, GSM9579, GSM9580, GSM9581, GSM9582, GSM9583, GSM9584, GSM9585, GSM9586, GSM9587, GSM9588, GSM9589, GSM9590, GSM9591, GSM9592, GSM9593, and GSM9594, which corresponded to three replicates for each time point (before and after treatment) and for four genotypes (Col, *arf7*, *arf19*, and *arf7arf19*). Independent normalizations for the respective data sets of Vanneste et al. (2005), Okushima et al. (2007), and De Smet et al. (2008) were performed using the robust multiarray average method (Irizarry et al., 2003). Differential analysis was performed with the moderated *t* test (Smyth, 2004) within the affylmGUI R package. Raw P values were adjusted by the Benjamini-Hochberg method to control the false discovery rate (Benjamini and Hochberg, 1995). A gene was declared differentially expressed if its adjusted P value was $\leq$0.01.The Affymetrix probe sets to Arabidopsis Genome Initiative ID assignment was done using the affy_ATH1_array_elements-2010-12-20.txt file downloaded from The Arabidopsis Information Resource (www.Arabidopsis.org).

In Vivo Root Confocal Imaging

For in vivo time-lapse confocal imaging, seedlings were placed into a Lab-Tek Chambered Borosilicate Coverglass System (NalgeNunc International) with a block of agar over the roots to keep the plants alive through visualization. All supplements were added during the preparation of the agar blocks. Time-lapse series were typically collected at 4-min intervals and for 7 to 15 h. For propidium iodide (PI) staining, seedlings were preincubated for 2 min in 10 μg/mL PI that was prepared in half-strength MS medium. Temperature and light were kept as constant as possible during all observations. Fluorescence imaging of roots was done with an Axiovert 100M confocal laser scanning microscope and LSM 510 version 3.2 software (Zeiss). For excitation of GFP, the 488-nm line of an argon laser was used, and PI was excited with the HeNe laser at 543 nm. GFP and PI were detected simultaneously by combining the settings indicated above in the sequential scanning facility of the microscope. Acquired images were quantitatively analyzed with ImageJ v1.34s software (http://rsbweb.nih.gov/ij/).

Real-Time PCR

RNA was extracted with the RNeasy kit (Qiagen). Poly(dT) cDNA was prepared from1 μg of total RNA with Superscript III reverse transcriptase (Invitrogen) and analyzed on an LightCycler 480 apparatus (Roche Diagnostics) with SYBR Green I Master kit (Roche Diagnostics) according to the manufacturer's instructions. All individual reactions were done in triplicate. Primer sequences are given in the Supplemental Table 3 online. For the expression analysis of transgenic lines, all values were normalized to the *ACTIN2* (At3g46520) gene. For the lateral root induction system, values were normalized against *ACTIN2* (At3g46520), *EF-1-α* (At5g60390), and *CDKA;1* (At3g48750). The delta cycle threshold (Ct) method was used for relative quantification of transcripts. All data represent the average of three biological replicates.

Histochemical and Histological Analysis

GUS staining was performed as described (Lammens et al., 2008). For microscopy analysis, samples were cleared by mounting in 90% lactic acid (Acros Organics) or as described previously (Malamy and Benfey, 1997). All samples were analyzed by differential interference contrast microscopy (Olympus BX51). Sections were prepared as described previously (De Smet et al., 2004).

Yeast One-Hybrid Analysis

Yeast strain YM4271 and destination vectors (pDEST-MW1 and pDEST-MW2) were obtained from Bart Deplancke (Deplancke et al., 2004). For the yeast one-hybrid cDNA library screen, promoter fragments of *E2Fa*, *E2Fb*, and *E2Fc* of 1364, 760, and 1997 bp, respectively, were used. Yeast reporter strains were designed as described previously (Deplancke et al., 2004). Yeast was handled and transformed according to the Yeast Protocol Handbook (Clontech). The cDNA yeast one-hybrid library screen was performed with a custom-made *Arabidopsis* cDNA library (Invitrogen). Transformation was according to the Yeast Protocol Handbook, except that 1.5 mL of 1$\times$ TE/1$\times$ LiAc was added to the competent yeast cells and that 20 μg of cDNA library was added together with 200 μL of carrier DNA (10 μg/μL) to the yeast-competent cells. Of a polyethylene glycol/LiAc solution, 20 mL was added, and the heat shock period at 42°C was extended to 20 min. All the yeast cells were plated on SD-His-Ura-Trp medium with 15 mM 3-aminotriazole. In total, 2.35×10^5 transformants were screened. Potential positives were selected after 6 to 8 d of incubation at 30°C, spotted onto an SD-His-Ura-Trp as well as an SD-His-Ura-Trp +3-aminotriazole plate for reanalysis of the positives, and tested for *LacZ* expression by a X-gal assay. For the positive candidates, the cDNA library plasmid inserts were amplified by PCR with primers specific for the cDNA library vector, sequenced, and analyzed by BLAST comparisons to identify the potential interactor (Altschul et al., 1997). Experimental background proteins were subtracted based on seven different yeast one-hybrid experiments.

ChIP and Quantitative PCR

The ChIP experiment was performed as described (Bowler et al., 2004), with minor modifications. One gram of tissue from 8-d-old plants was harvested and immersed in 1% formaldehyde under vacuum for 10 min. Gly was added to a final concentration of 0.125 M, and incubation was continued for 5 min. After washing, the nuclei were isolated, and cross-linked DNA/protein complexes were fragmented by sonication with a Bioruptor sonicator (Diagenode), resulting in fragments of $\sim$500 bp. After centrifugation (16,000*g*), the supernatant was precleared with 40 μL of salmon sperm DNA/protein agarose (Millipore). Of the supernatant, 10 μL was used as input, while the rest was divided into two samples, of which one sample was treated with 10 μL anti-GFP antibody (Rockland) and the other with no antibody. The samples were incubated overnight. Immunoprecipitates were collected with 40 μL of salmon sperm DNA/protein Agarose (Millipore) and subsequently eluted from the beads. All centrifugation steps with bead-containing samples were done at 1000*g*.

Proteins were de-cross-linked, and DNA was purified by phenol/chloroform/isoamyl alcohol extraction and ethanol precipitation. Pellets were resuspended in 40 μL of Tris-EDTA buffer (0.05 M Tris-HCl and 0.02 M EDTA, pH 8). The concentration of DNA purified by ChIP was measured with the Quant-iT ds-DNA HS assay kit (Invitrogen), and each sample was diluted for the quantitative PCR at the same starting concentration. The SYBR Green I Master kit (Roche Diagnostics) was used for all the quantitative PCRs. *ACTIN2* and promoter regions of *DEL1* and *E2Fc* were used as negative controls. The approach used to analyze the quantitative PCR data was %INPUT ($100*2^{(Ct[Input] - Ct[IP])}$). Primers are given in Supplemental Table 3 online. ChIP data were obtained from single experiments, but similar data were acquired from independent runs.

FRET

The LBD-fluorophore fusions created with LBD18 (At2g45420) and LBD33 (At5g06080), the transient transformation of *Nicotiana benthamiana* plants, the confocal microscopy, and FRET measurements were performed as described previously (Bleckmann et al., 2010). Transgene expression was induced 24 h after infiltration and analyzed within 16 to 18 h. A region surrounding the nucleus was bleached after five detection frames with 100% laser intensity of the 561-nm diode and 120 iterations. Fifteen frames were recorded after photobleaching. The GFP fluorescence intensity change was analyzed in a region of interest within the nucleus. Only measurements with <10% GFP intensity fluctuations before acceptor bleaching were further analyzed. The percentage change of the GFP intensity directly before and after bleaching was analyzed as E_{FRET} = (GFPafter − GFPbefore)/GFPafter × 100. A minimum of 15 measurements was performed for each experiment. Significance was analyzed with a Student's *t* test.

TAP

Arabidopsis cell suspension cultures (PSB-D, this laboratory) were transformed as described previously with *LBD18* fused to the Protein G/streptavidin binding peptide (GS)-TAP tag (Van Leene et al., 2007). TAP of protein complexes was done with the GS tag (Bürckstümmer et al., 2006) followed by protein precipitation and separation as described (Van Leene et al., 2008). Proteolysis and peptide isolation, acquisition of mass spectra by a 4800 Proteomics Analyzer (Applied Biosystems), and mass spectrometry–based protein homology identification based on the TAIR 8 genomic database were performed as described (Van Leene et al., 2010). Experimental background proteins were subtracted based on 40 TAP experiments on wild-type cultures and cultures producing TAP-tagged mock proteins GUS, red fluorescent protein, and GFP (Van Leene et al., 2010).

Transient Expression Assays

Assays for transient expression were done as described previously (De Sutter et al., 2005). Briefly, protoplasts were prepared from a Bright Yellow-2 tobacco cell culture (Nagata et al., 1992) and cotransfected with a reporter plasmid containing the *Firefly luciferase* (*fLUC*) reporter gene driven by the *E2Fa* promoter, a normalization construct expressing *Renilla luciferase* (*rLUC*) under control of the *35S* promoter, and effector constructs. For the *ProE2Fa*:*LUC* reporter construct, the *pEN-L4-ProE2Fa-R1* vector, also used for cloning yeast one-hybrid vectors, was recombined together with *pEN-L1-fLUC-L2* by multisite Gateway LR cloning with pm42GW7 (Karimi et al., 2007). For the effector constructs, *pEN-L1-ORF-R2* (ORFs representing *LBD18*, *LBD18-SRDX*, *LBD18-VP16*, and *LBD33*) were used to introduce the ORFs by Gateway LR cloning into p2GW7. *LBD18-SRDX* was generated by PCR, adding the SRDX coding sequence to the cDNA_LBD18_RV primer. For *LBD18-VP16*, coding regions of both *LBD18* and *VP16* were amplified and fused by ligation-mediated PCR with the chimeric_LBD18_VP16 primer. For each experiment, 2 μg of each plasmid and the *p2GW7-GUS* mock effector plasmid were used to equalize the total effector amount. After transfection, protoplasts were incubated overnight and then lysed. fLUC and rLUC activities were determined with the Dual-Luciferase reporter assay system (Promega). Variations in transfection efficiency and technical errors were corrected by normalization of fLUC by rLUC activities.

Accession Numbers

Sequence data from this article can be found in the Arabidopsis Genome Initiative or GenBank/EMBL databases under the following accession numbers: LBD18, At2g45420; LBD33, At5g06080; and E2Fa, At2g36010. Sequence data for the T-DNA insertion lines are as follows: SALK_038125 (*lbd18-1*), SAIL_269_H02 (*lbd18-2*), SAIL_95_H10 (*lbd33*), GABI_348E09 (*e2fa-2*), MPIZ-244 (*e2fa-1*), and SALK_103138 (*e2fb*).

Supplemental Data

The following materials are available in the online version of this article.

Supplemental Figure 1. E2Fa Regulates Lateral Root Initiation.

Supplemental Figure 2. Schematic Representation of the Localization of Putative LBD Binding Sites and the Primers Used for ChIP-Quantitative PCR.

Supplemental Figure 3. *LBD18* and *LBD33* Auxin Induction in Roots Is Dependent on the SLR/ARF7/ARF19 Pathway.

Supplemental Figure 4. E2Fb-GFP Protein Levels upon NAA Application in Xylem-Pole Pericycle Cells.

Supplemental Figure 5. Numbers of Lateral Roots of an *e2fb* Mutant.

Supplemental Figure 6. Numbers of Lateral Roots of *lbd18*, *lbd33*, and *lbd18 lbd33* Mutants.

Supplemental Table 1. Primers Used for Genotyping.

Supplemental Table 2. Primers Used for Cloning.

Supplemental Table 3. Primers Used for RT-PCR.

ACKNOWLEDGMENTS

We thank Martine De Cock and Annick Bleys for help in preparing the manuscript. This work was supported by a grant from the Interuniversity Attraction Poles Programme (IUAPVI/33), initiated by the Belgian State, Science Policy Office. B.B. is grateful to the Agency for Innovation by Science and Technology in Flanders for a predoctoral fellowship.

AUTHOR CONTRIBUTIONS

B.B., C.K., G.D.J., J.F., R.S., T.B., and L.D.V. designed the research. B.B., V.V., S.P.C.S., S.M., B.P., S.N., C.L.A.K., and G.P. performed the research. B.B., B.P., G.D.J., R.S., T.B., and L.D.V. analyzed data. Z.M. and L.B. contributed reagents, materials, and analysis tools. B.B. and L.D.V. wrote the article.

Received June 17, 2011; revised September 12, 2011; accepted October 2, 2011; published October 14, 2011.

REFERENCES

Altschul, S.F., Madden, T.L., Schäffer, A.A., Zhang, J., Zhang, Z., Miller, W., and Lipman, D.J. (1997). Gapped BLAST and PSI-BLAST: A new generation of protein database search programs. Nucleic Acids Res. **25:** 3389–3402.

Benjamini, Y., and Hochberg, Y. (1995). Controlling the false discovery rate: A practical and powerful approach to multiple testing. J. R. Stat. Soc. Series B Stat. Methodol. **57:** 289–300.

Benková, E., Michniewicz, M., Sauer, M., Teichmann, T., Seifertová, D., Jürgens, G., and Friml, J. (2003). Local, efflux-dependent auxin gradients as a common module for plant organ formation. Cell **115:** 591–602.

Berckmans, B., and De Veylder, L. (2009). Transcriptional control of the cell cycle. Curr. Opin. Plant Biol. **12:** 599–605.

Bleckmann, A., Weidtkamp-Peters, S., Seidel, C.A.M., and Simon, R. (2010). Stem cell signaling in Arabidopsis requires CRN to localize CLV2 to the plasma membrane. Plant Physiol. **152:** 166–176.

Borghi, L., Bureau, M., and Simon, R. (2007). *Arabidopsis JAGGED LATERAL ORGANS* is expressed in boundaries and coordinates *KNOX* and *PIN* activity. Plant Cell **19:** 1795–1808.

Bowler, C., Benvenuto, G., Laflamme, P., Molino, D., Probst, A.V., Tariq, M., and Paszkowski, J. (2004). Chromatin techniques for plant cells. Plant J. **39:** 776–789.

Bürckstümmer, T., Bennett, K.L., Preradovic, A., Schütze, G., Hantschel, O., Superti-Furga, G., and Bauch, A. (2006). An efficient tandem affinity purification procedure for interaction proteomics in mammalian cells. Nat. Methods **3:** 1013–1019.

Bureau, M., Rast, M.I., Illmer, J., and Simon, R. (2010). *JAGGED LATERAL ORGAN* (*JLO*) controls auxin dependent patterning during development of the *Arabidopsis* embryo and root. Plant Mol. Biol. **74:** 479–491.

Bureau, M., and Simon, R. (2008). *JLO* regulates embryo patterning and organ initiation by controlling auxin transport. Plant Signal. Behav. **3:** 145–147.

Casimiro, I., Marchant, A., Bhalerao, R.P., Beeckman, T., Dhooge, S., Swarup, R., Graham, N., Inzé, D., Sandberg, G., Casero, P.J., and Bennett, M. (2001). Auxin transport promotes *Arabidopsis* lateral root initiation. Plant Cell **13:** 843–852.

Chalfun-Junior, A., Franken, J., Mes, J.J., Marsch-Martinez, N., Pereira, A., and Angenent, G.C. (2005). *ASYMMETRIC LEAVES2-LIKE1* gene, a member of the AS2/LOB family, controls proximal-distal patterning in *Arabidopsis* petals. Plant Mol. Biol. **57:** 559–575.

Clough, S.J., and Bent, A.F. (1998). Floral dip: A simplified method for *Agrobacterium*-mediated transformation of *Arabidopsis thaliana*. Plant J. **16:** 735–743.

del Pozo, J.C., Boniotti, M.B., and Gutierrez, C. (2002). Arabidopsis E2Fc functions in cell division and is degraded by the ubiquitin-SCF^{AtSKP2} pathway in response to light. Plant Cell **14:** 3057–3071.

del Pozo, J.C., Diaz-Trivino, S., Cisneros, N., and Gutierrez, C. (2006). The balance between cell division and endoreplication depends on E2FC-DPB, transcription factors regulated by the ubiquitin-SCF^{SKP2A} pathway in *Arabidopsis*. Plant Cell **18:** 2224–2235.

Deplancke, B., Dupuy, D., Vidal, M., and Walhout, A.J.M. (2004). A Gateway-compatible yeast one-hybrid system. Genome Res. **14:** 2093–2101.

De Rybel, B., et al. (2010). A novel Aux/IAA28 signaling cascade activates GATA23-dependent specification of lateral root founder cell identity. Curr. Biol. **20:** 1697–1706.

De Smet, I., Chaerle, P., Vanneste, S., De Rycke, R., Inzé, D., and Beeckman, T. (2004). An easy and versatile embedding method for transverse sections. J. Microsc. **213:** 76–80.

De Smet, I., et al. (2010). Bimodular auxin response controls organogenesis in *Arabidopsis*. Proc. Natl. Acad. Sci. USA **107:** 2705–2710.

De Smet, I., et al. (2007). Auxin-dependent regulation of lateral root positioning in the basal meristem of *Arabidopsis*. Development **134:** 681–690.

De Smet, I., et al. (2008). Receptor-like kinase ACR4 restricts formative cell divisions in the *Arabidopsis* root. Science **322:** 594–597.

De Smet, I., et al. (2011). Unraveling the evolution of auxin signaling. Plant Physiol. **155:** 209–221.

De Sutter, V., Vanderhaeghen, R., Tilleman, S., Lammertyn, F., Vanhoutte, I., Karimi, M., Inzé, D., Goossens, A., and Hilson, P. (2005). Exploration of jasmonate signalling via automated and standardized transient expression assays in tobacco cells. Plant J. **44:** 1065–1076.

De Veylder, L., Beeckman, T., Beemster, G.T.S., de Almeida Engler, J., Ormenese, S., Maes, S., Naudts, M., Van Der Schueren, E., Jacqmard, A., Engler, G., and Inzé, D. (2002). Control of proliferation, endoreduplication and differentiation by the *Arabidopsis* E2Fa-DPa transcription factor. EMBO J. **21:** 1360–1368.

Esmon, C.A., Tinsley, A.G., Ljung, K., Sandberg, G., Hearne, L.B., and Liscum, E. (2006). A gradient of auxin and auxin-dependent transcription precedes tropic growth responses. Proc. Natl. Acad. Sci. USA **103:** 236–241.

Evans, M.M. (2007). The *indeterminate gametophyte1* gene of maize encodes a LOB domain protein required for embryo sac and leaf development. Plant Cell **19:** 46–62.

Friml, J. (2003). Auxin transport - Shaping the plant. Curr. Opin. Plant Biol. **6:** 7–12.

Friml, J., Wiśniewska, J., Benková, E., Mendgen, K., and Palme, K. (2002). Lateral relocation of auxin efflux regulator PIN3 mediates tropism in *Arabidopsis*. Nature **415:** 806–809.

Fuchs, I., Philippar, K., Ljung, K., Sandberg, G., and Hedrich, R. (2003). Blue light regulates an auxin-induced K^+-channel gene in the maize coleoptile. Proc. Natl. Acad. Sci. USA **100:** 11795–11800.

Fukaki, H., Tameda, S., Masuda, H., and Tasaka, M. (2002). Lateral root formation is blocked by a gain-of-function mutation in the *SOLITARY-ROOT/IAA14* gene of *Arabidopsis*. Plant J. **29:** 153–168.

Henriques, R., Magyar, Z., Monardes, A., Khan, S., Zalejski, C., Orellana, J., Szabados, L., de la Torre, C., Koncz, C., and Bögre, L. (2010). *Arabidopsis* S6 kinase mutants display chromosome instability and altered RBR1-E2F pathway activity. EMBO J. **29:** 2979–2993.

Himanen, K., Boucheron, E., Vanneste, S., de Almeida Engler, J., Inzé, D., and Beeckman, T. (2002). Auxin-mediated cell cycle activation during early lateral root initiation. Plant Cell **14:** 2339–2351.

Himanen, K., Vuylsteke, M., Vanneste, S., Vercruysse, S., Boucheron, E., Alard, P., Chriqui, D., Van Montagu, M., Inzé, D., and Beeckman, T. (2004). Transcript profiling of early lateral root initiation. Proc. Natl. Acad. Sci. USA **101:** 5146–5151.

Husbands, A., Bell, E.M., Shuai, B., Smith, H.M.S., and Springer, P.S. (2007). LATERAL ORGAN BOUNDARIES defines a new family of DNA-binding transcription factors and can interact with specific bHLH proteins. Nucleic Acids Res. **35:** 6663–6671.

Inzé, D., and De Veylder, L. (2006). Cell cycle regulation in plant development. Annu. Rev. Genet. **40:** 77–105.

Irizarry, R.A., Hobbs, B., Collin, F., Beazer-Barclay, Y.D., Antonellis, K.J., Scherf, U., and Speed, T.P. (2003). Exploration, normalization, and summaries of high density oligonucleotide array probe level data. Biostatistics **4:** 249–264.

Iwakawa, H., Iwasaki, M., Kojima, S., Ueno, Y., Soma, T., Tanaka, H., Semiarti, E., Machida, Y., and Machida, C. (2007). Expression of the *ASYMMETRIC LEAVES2* gene in the adaxial domain of Arabidopsis leaves represses cell proliferation in this domain and is critical for the development of properly expanded leaves. Plant J. **51:** 173–184.

Karimi, M., Depicker, A., and Hilson, P. (2007). Recombinational cloning with plant gateway vectors. Plant Physiol. **145:** 1144–1154.

Karimi, M., Inzé, D., and Depicker, A. (2002). GATEWAY vectors for *Agrobacterium*-mediated plant transformation. Trends Plant Sci. **7:** 193–195.

Kang, J., Mizukami, Y., Wang, H., Fowke, L., and Dengler, N.G. (2007). Modification of cell proliferation patterns alters leaf vein architecture in *Arabidopsis thaliana*. Planta **226:** 1207–1218.

Lammens, T., Boudolf, V., Kheibarshekan, L., Zalmas, L.P., Gaamouche, T., Maes, S., Vanstraelen, M., Kondorosi, E., La Thangue, N.B., Govaerts, W., Inzé, D., and De Veylder, L. (2008). Atypical E2F activity restrains APC/$C^{CCS52A2}$ function obligatory for endocycle onset. Proc. Natl. Acad. Sci. USA **105:** 14721–14726.

Lee, H.W., Kim, N.Y., Lee, D.J., and Kim, J. (2009). *LBD18/ASL20* regulates lateral root formation in combination with *LBD16/ASL18* downstream of *ARF7* and *ARF19* in Arabidopsis. Plant Physiol. **151:** 1377–1389.

Lin, W.C., Shuai, B., and Springer, P.S. (2003). The *Arabidopsis LATERAL ORGAN BOUNDARIES*-domain gene *ASYMMETRIC LEAVES2* functions in the repression of *KNOX* gene expression and in adaxial-abaxial patterning. Plant Cell **15:** 2241–2252.

Majer, C., and Hochholdinger, F. (2011). Defining the boundaries: Structure and function of LOB domain proteins. Trends Plant Sci. **16:** 47–52.

Malamy, J.E., and Benfey, P.N. (1997). Organization and cell differentiation in lateral roots of *Arabidopsis thaliana*. Development **124:** 33–44.

Matsumura, Y., Iwakawa, H., Machida, Y., and Machida, C. (2009). Characterization of genes in the *ASYMMETRIC LEAVES2/LATERAL ORGAN BOUNDARIES* (*AS2/LOB*) family in *Arabidopsis thaliana*, and functional and molecular comparisons between *AS2* and other family members. Plant J. **58:** 525–537.

Moreno-Risueno, M.A., Van Norman, J.M., Moreno, A., Zhang, J., Ahnert, S.E., and Benfey, P.N. (2010). Oscillating gene expression determines competence for periodic *Arabidopsis* root branching. Science **329:** 1306–1311.

Nagata, T., Nemoto, Y., and Hasezawa, S. (1992). Tobacco BY-2 cell line as the "HeLa" cell in the cell biology of higher plants. Int. Rev. Cytol. **132:** 1–30.

Oh, S.A., Park, K.S., Twell, D., and Park, S.K. (2010). The *SIDECAR POLLEN* gene encodes a microspore-specific LOB/AS2 domain protein required for the correct timing and orientation of asymmetric cell division. Plant J. **64:** 839–850.

Okushima, Y., Fukaki, H., Onoda, M., Theologis, A., and Tasaka, M. (2007). ARF7 and ARF19 regulate lateral root formation via direct activation of *LBD/ASL* genes in *Arabidopsis*. Plant Cell **19:** 118–130.

Okushima, Y., et al. (2005). Functional genomic analysis of the *AUXIN RESPONSE FACTOR* gene family members in *Arabidopsis thaliana*: Unique and overlapping functions of *ARF7* and *ARF19*. Plant Cell **17:** 444–463.

Overvoorde, P., Fukaki, H., and Beeckman, T. (2010). Auxin control of root development. Cold Spring Harb. Perspect. Biol. **2:** a001537.

Parizot, B., De Rybel, B., and Beeckman, T. (2010). VisuaLRTC: A new view on lateral root initiation by combining specific transcriptome data sets. Plant Physiol. **153:** 34–40.

Péret, B., De Rybel, B., Casimiro, I., Benková, E., Swarup, R., Laplaze, L., Beeckman, T., and Bennett, M.J. (2009). *Arabidopsis* lateral root development: An emerging story. Trends Plant Sci. **14:** 399–408.

Ramirez-Parra, E., López-Matas, M.A., Fründt, C., and Gutierrez, C. (2004). Role of an atypical E2F transcription factor in the control of *Arabidopsis* cell growth and differentiation. Plant Cell **16:** 2350–2363.

Ríos, G., et al. (2002). Rapid identification of *Arabidopsis* insertion mutants by non-radioactive detection of T-DNA tagged genes. Plant J. **32:** 243–253.

Rolland-Lagan, A.-G. (2008). Vein patterning in growing leaves: Axes and polarities. Curr. Opin. Genet. Dev. **18:** 348–353.

Sanz, L., et al. (2011). The *Arabidopsis* D-type cyclin CYCD2;1 and the inhibitor ICK2/KRP2 modulate auxin-induced lateral root formation. Plant Cell **23:** 641–660.

Semiarti, E., Ueno, Y., Tsukaya, H., Iwakawa, H., Machida, C., and Machida, Y. (2001). The *ASYMMETRIC LEAVES2* gene of *Arabidopsis thaliana* regulates formation of a symmetric lamina, establishment of venation and repression of meristem-related homeobox genes in leaves. Development **128:** 1771–1783.

Shuai, B., Reynaga-Peña, C.G., and Springer, P.S. (2002). The *lateral organ boundaries* gene defines a novel, plant-specific gene family. Plant Physiol. **129:** 747–761.

Smyth, G.K. (2004). Linear models and empirical Bayes methods for assessing differential expression in microarray experiments. Stat. Appl. Genet. Mol. Biol. **3:** Article 3.

Soyano, T., Thitamadee, S., Machida, Y., and Chua, N.-H. (2008). *ASYMMETRIC LEAVES2-LIKE19/LATERAL ORGAN BOUNDARIES DOMAIN30* and *ASL20/LBD18* regulate tracheary element differentiation in *Arabidopsis*. Plant Cell **20:** 3359–3373.

Sozzani, R., Maggio, C., Varotto, S., Canova, S., Bergounioux, C., Albani, D., and Cella, R. (2006). Interplay between Arabidopsis activating factors E2Fb and E2Fa in cell cycle progression and development. Plant Physiol. **140:** 1355–1366.

Tanaka, H., Dhonukshe, P., Brewer, P.B., and Friml, J. (2006). Spatiotemporal asymmetric auxin distribution: a means to coordinate plant development. Cell. Mol. Life Sci. **63:** 2738–2754.

Traas, J., and Monéger, F. (2010). Systems biology of organ initiation at the shoot apex. Plant Physiol. **152:** 420–427.

Vanneste, S., and Friml, J. (2009). Auxin: A trigger for change in plant development. Cell **136:** 1005–1016.

Vanneste, S., et al. (2005). Cell cycle progression in the pericycle is not sufficient for SOLITARY ROOT/IAA14-mediated lateral root initiation in *Arabidopsis thaliana*. Plant Cell **17:** 3035–3050.

Van Leene, J., et al. (2010). Targeted interactomics reveals a complex core cell cycle machinery in *Arabidopsis thaliana*. Mol. Syst. Biol. **6:** 397.

Van Leene, J., et al. (2007). A tandem affinity purification-based technology platform to study the cell cycle interactome in *Arabidopsis thaliana*. Mol. Cell. Proteomics **6:** 1226–1238.

Van Leene, J., Witters, E., Inzé, D., and De Jaeger, G. (2008). Boosting tandem affinity purification of plant protein complexes. Trends Plant Sci. **13:** 517–520.

Vlieghe, K., Boudolf, V., Beemster, G.T.S., Maes, S., Magyar, Z., Atanassova, A., de Almeida Engler, J., De Groodt, R., Inzé, D., and De Veylder, L. (2005). The DP-E2F-like gene *DEL1* controls the endocycle in *Arabidopsis thaliana*. Curr. Biol. **15:** 59–63.

Wilmoth, J.C., Wang, S., Tiwari, S.B., Joshi, A.D., Hagen, G., Guilfoyle, T.J., Alonso, J.M., Ecker, J.R., and Reed, J.W. (2005). NPH4/ARF7 and ARF19 promote leaf expansion and auxin-induced lateral root formation. Plant J. **43:** 118–130.

Zgurski, J.M., Sharma, R., Bolokoski, D.A., and Schultz, E.A. (2005). Asymmetric auxin response precedes asymmetric growth and differentiation of *asymmetric leaf1* and *asymmetric leaf2* Arabidopsis leaves. Plant Cell **17:** 77–91.